Engineering Notes

ENGINEERING NOTES are short manuscripts describing new developments or important results of a preliminary nature. These Notes cannot exceed 6 manuscript pages and 3 figures; a page of text may be substituted for a figure and vice versa. After informal review by the editors, they may be published within a few months of the date of receipt. Style requirements are the same as for regular contributions (see inside back cover).

AIAA 82-4217

Minimum Induced Drag of Canard Configurations

Ilan M. Kroo*
Stanford University, Stanford, California

Nomenclature

A_n = Fourier coefficient in wing lift distribution
$\bar{A}_n$ = nondimensionalized Fourier coefficient, $A_n/A_1 = A_n/L_w$
b = span
$\bar{b}$ = ratio of smaller span to larger span = b_c/b_w
D_i = induced drag
e = induced drag factor
e_1, e_2, e_3 = self-induced and interference drag factors from Ref. 2
h = vertical distance between wing and canard
$\bar{h}$ = nondimensional vertical gap = $2h/b_c$
I_n = definite integral given in Eq. (5)
L = lift
$\bar{L}$ = lift ratio = L_c/L_w
l = section lift
q = dynamic pressure
w = downwash velocity
w_0 = downwash at canard root induced by canard trailing vortex system
y = spanwise coordinate
$\bar{y}$ = nondimensional spanwise coordinate = $2y/b_w$
σ = Prandtl's interference factor
σ_* = nonelliptic interference factor
θ = spanwise angular coordinate = $\cos^{-1}\bar{y}$

Subscripts

w = wing (or larger span)
c = canard or tail

Introduction

THE quest for energy-efficient aircraft has led to a recent resurgence of interest in canard configurations and a need for practical drag estimation methods for use in the preliminary design of such aircraft. In the context of preliminary design optimization, modern panel codes may prove prohibitively time-consuming and expensive. A large gap exists between these refined methods and the biplane equation of Prandtl,[1] which is also widely used because of its simplicity:

$$D_i = \frac{L_w^2}{q\pi b_w^2} + \frac{2L_cL_w\sigma}{q\pi b_c b_w} + \frac{L_c^2}{q\pi b_c^2} \tag{1}$$

The limited number of variables and algebraic form of Eq. (1) (where σ is a function of span and vertical gap ratios only) make it particularly useful. Many recent analyses[2-5] of trimmed drag for conventional and canard designs and of optimum center of gravity position have been based on this equation and reflect the utility of such a simple approach.

The key assumption underlying Eq. (1) is that each surface is elliptically loaded. However, when operating in the downwash field of a highly loaded canard, the wing's lift distribution tends to be shifted outboard because of the downwash directly behind, and upwash outboard, of the canard. The wing, of course, could be twisted to produce an elliptic load distribution in spite of this nonuniform downwash field, but, despite some confusion in the literature, the idealized individually elliptic load distribution is often far from ideal (Fig. 1). This is easily demonstrated in the case when the two surfaces are coplanar. Prandtl pointed out that, in this case, Munk's stagger theorem[6] permitted superposition of the individual loadings so that the system could be treated as a single wing for the purposes of induced drag calculation. The minimum induced drag is achieved when the *total* loading is elliptical over the larger span; the *wing's* lift distribution is decreased inboard and increased outboard of the canard. This loading is in the same sense that the lift distribution of an untwisted wing is shifted when operating in the canard's downwash field and the loading change probably accounts for the overestimation of canard drag by Eq. (1) when compared with experiments.[7]

Because of the limitation of Eq. (1) to elliptically loaded wings, several attempts have been made to generalize the expression to include more realistic distributions. Reid[8] suggests adding coefficients to the first and third terms in Eq. (1) to account for the increase in "self-induced drag" for nonelliptic wings while leaving the interference drag term unchanged.

Laitone[9] writes

$$D_i = \frac{L_w^2}{q\pi b_w^2 e_1} + \frac{2L_cL_w\sigma}{q\pi b_c b_w e_3} + \frac{L_c^2}{q\pi b_c^2 e_2} \tag{2}$$

with $e_1, e_2 < 1$ reflecting the self-induced drag of an isolated nonelliptical wing, while e_3 is obtained by integration of Trefftz-plane downwash. Laitone determined these constants only for the case of uniform (constant) loading on each span.

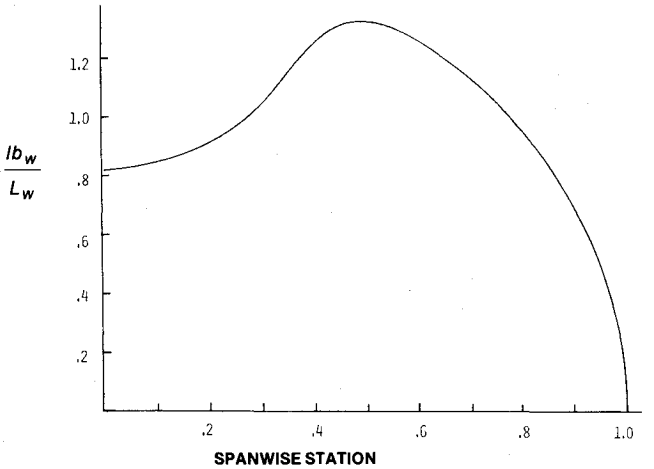

Fig. 1 Wing lift distribution for minimum induced drag with elliptically loaded canard; $2h/b_c = 0.2$, $\bar{L} = 0.2$, $\bar{b} = 0.4$.

Received Nov. 2, 1981; revision received May 6, 1982.

*Graduate Student, Department of Aeronautics and Astronautics.

Approximate Approach

The assumption of elliptic load distributions is reasonable when the vertical gap, h, is large or when the surfaces have equal spans. [The minimum induced drag for equal span biplanes is computed by conformal mappings in Ref. 10 (pp. 216-221) and is essentially that given by Eq. (1).] As mentioned previously, the wing load distribution for minimum induced drag of a canard aircraft with small gap and canard span is greatly distorted from elliptical. The distribution of lift on the canard, however, is not distorted greatly since the downwash field produced by the wing in this area is more uniform. (Similarly, the lift distribution on a tail of significantly smaller span than the wing is not far from elliptical.) Thus it seems that the assumption of elliptic loading on the larger span is most responsible for the differences between Eq. (1) and the actual induced drag. By assuming that the smaller span is elliptically loaded, the lift distribution on the larger span for minimum induced drag may be determined directly.†

Derivation

Applying the general theorems of Munk,[6] the system may be treated as an unstaggered biplane for which the drag of one surface produced by the downwash of the second surface is equal to that part of the second surface's drag induced by the downwash of the first. If the smaller span, b_c, is elliptically loaded and the section lift of the wing is represented by the Fourier series,

$$l = \frac{4}{\pi b_w} \sum_{\text{odd}} A_n \sin n\theta$$

with $y = (b_w/2)\cos\theta$, the spanwise coordinate, then

$$D_i = \frac{L_w^2 \sigma_2}{q\pi b_w^2} + \frac{2L_c L_w \sigma_1}{q\pi b_c b_w} + \frac{L_c^2}{q\pi b_c^2} \tag{3}$$

which is Eq. (2) with the factor $e_2 = 1$ for the elliptically loaded canard, and with

$$\sigma_2 = \sum_{\text{odd}} n\bar{A}_n^2 \qquad \bar{A}_n \equiv A_n/A_1 = A_n/L_w \tag{4}$$

the well-known result for an isolated finite wing, and

$$\sigma_1 = \frac{4b_w}{\pi b_c} \sum_{\text{odd}} \bar{A}_n \int_0^1 \frac{w(y)}{w_0} \sin n(\cos^{-1}\bar{y})\, d\bar{y} \tag{5}$$

The downwash induced on the wing by the canard for this unstaggered system is given by von Kármán and Burgers (Ref. 10, p. 148):

$$w/w_0 = 1 - Re\{\xi/\sqrt{\xi^2 - 1}\}$$

with $\xi = 2y/b_c + i2h/b_c$ and $w_0 =$ downwash at the canard root, so

$$\sigma_1 = (4b_w/\pi b_c) \sum_{\text{odd}} \bar{A}_n I_n \tag{6}$$

where $I_n[(b_c/b_w), (h/b_c)]$ is the definite integral in Eq. (5). Thus, if the lift distribution of the larger span is given, the induced drag may be computed from Eqs. (3), (4), and (6).

We can, moreover, solve for the wing lift distribution which results in minimum induced drag for given L_c and L_w.

†A similar approach, with higher order components of the smaller span's load distribution, leads to a more general solution which differs little from that given here but has the disadvantage that additional interference constants are required, and the constants are expressed, not explicitly, but as the solution to a linear system.

Setting

$$\frac{\partial D_i}{\partial A_j} = 0 \qquad j = 3,5,7,\ldots$$

yields

$$\bar{A}_j = -4\bar{L} I_j/\pi \bar{b}^2 j \qquad j = 3,5,7,\ldots \tag{7}$$

Thus, from Eq. (6),

$$\sigma_1 = \frac{4}{\pi \bar{b}} \left[I_1 - \frac{4\bar{L}}{\pi \bar{b}^2} \sum_{\substack{\text{odd} \\ n>1}} \frac{I_n^2}{n} \right] \tag{8}$$

and from Eq. (4)

$$\sigma_2 = 1 + \frac{16\bar{L}^2}{\pi^2 \bar{b}^4} \sum_{\substack{\text{odd} \\ n>1}} \frac{I_n^2}{n} \tag{9}$$

Substitution into Eq. (3) finally produces

$$D_i = \frac{L_w^2}{q\pi b_w^2} + \frac{2L_c L_w \sigma}{q\pi b_c b_w} + \frac{L_c^2 \sigma_*}{q\pi b_c^2} \tag{10}$$

where

$$\sigma = 4I_1/\pi \bar{b} \tag{11}$$

and

$$\sigma_* = 1 - \frac{16}{\pi^2 \bar{b}^2} \sum_{\substack{\text{odd} \\ n>1}} \frac{I_n^2}{n} \le 1 \tag{12}$$

Equation (10) is identical with Eq. (1) except for the addition of the coefficient σ_* in the last term. It is interesting to compare Eq. (10) with the original expression (3), in which the coefficients σ_1, σ_2 are constant with the ratio $L_c/L_w \equiv \bar{L}$ only if the shape of the lift distribution is fixed. When the shape of the lift distribution is allowed to vary with $\bar{L}$, but required to produce minimum induced drag, Eq. (10) holds with σ and σ_* independent of $\bar{L}$. Unlike Eq. (3), in which the three terms consist of two self-induced drag terms and an interference

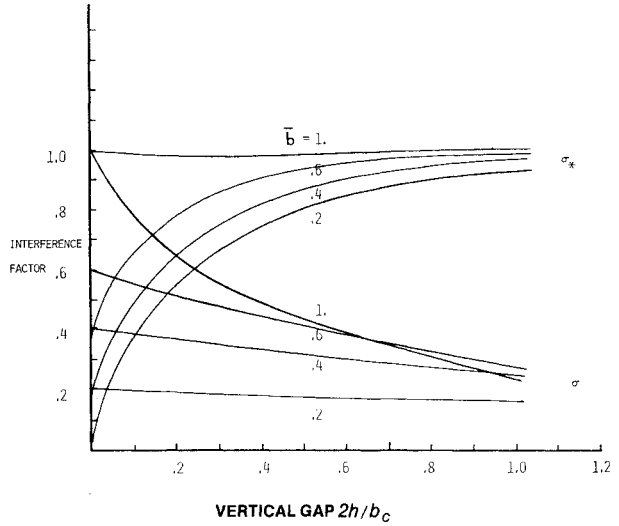

Fig. 2 Interference factors [Eq. (10)].

term, all three terms of Eq. (10) contain both self-induced and interference effects.

Discussion

The value of σ is tabulated and presented graphically in Ref. 10 (pp. 217,218); it is reproduced here along with the new constant σ_* in Fig. 2. σ_* reflects the extent to which the momentum imparted to a small mass of air by the canard may be redistributed by the wing over a larger mass of air. Thus, when $h=0$, the wing is capable of redistributing the momentum over its entire span so that the minimum induced drag (regardless of canard load) is just that which would be produced by a single elliptically loaded wing carrying the total lift. This explains the interesting result that for many cases the interference terms are beneficial and the induced drag is actually lower than if the two wings were infinitely far apart. Equation (1), to the contrary, suggests that induced drag decreases with larger vertical gap whenever $\bar{L}>0$.

The ratio of the system's minimum induced drag to that of a monoplane with the span of the wing and carrying the same total lift is

$$\frac{1}{e}=\frac{1+2\sigma\bar{L}/\bar{b}+\sigma_*\bar{L}^2/\bar{b}^2}{(1+\bar{L})^2} \tag{13}$$

Since $\sigma_*=1$ when the wing is elliptically loaded, the minimum induced drag given by Eq. (10) may differ significantly from that given by Eq. (1). If, for example, $2h/b_c=0.2$, $L_c/L_w=0.3$, and $b_c/b_w=0.4$, Eq. (13) gives $e=0.885$, while, if the surfaces were elliptically loaded, $e=0.802$. Differences become larger for smaller gaps and larger span loading ratios, $\bar{L}/\bar{b}$. Thus, although Eq. (13) may be used for estimating the induced drag of conventional, aft-tail configurations, it is especially useful for canard configurations which, because of stability and trim constraints, generally require larger values of $\bar{L}/\bar{b}$.

Figure 2 illustrates the rapid variation of σ_* for small vertical gaps. This decrease in σ_* reflects the substantial reduction in induced drag compared with the elliptically loaded case. Because of this sensitivity, however, the theoretical result that $e=1$ and is independent of $\bar{L}$ when no vertical gap is present is not achievable in practical cases where h does not vanish completely.

References

[1] Prandtl, L., "Induced Drag of Multiplanes," NACA TN-182, March 1924.

[2] Laitone, E., "Positive Tail Loads for Minimum Induced Drag of Subsonic Aircraft," *Journal of Aircraft,* Vol. 15, Dec. 1978, pp. 837-842.

[3] Wolkovitch, J., "Subsonic V/STOL Configurations with Tandem Wings," *Journal of Aircraft,* Vol. 16, Sept. 1979, pp. 605-611.

[4] McLaughlin, M., "Calculations, and Comparison with an Ideal Minimum of Trimmed Drag for Conventional and Canard Configurations Having Various Levels of Static Stability," NASA TN-D-8391, 1977.

[5] Sachs, G., "Minimum Trimmed Drag and Optimum C.G. Position," *Journal of Aircraft,* Vol. 15, Aug. 1978, pp. 456-459.

[6] Munk, M., "Minimum Induced Drag of Airfoils," NACA Report 121, 1921.

[7] Feistal, T., Corsiglia, V., and Levin, D., "Wind-Tunnel Measurements of Wing-Canard Interference and a Comparison with Various Theories," SAE Technical Paper 810575, April 1981.

[8] Reid, E.G., *Applied Wing Theory,* McGraw-Hill, New York, 1932.

[9] Laitone, E., "Prandtl's Biplane Theory Applied to Canard and Tandem Aircraft," *Journal of Aircraft,* Vol. 17, April 1980, pp. 233-237.

[10] von Kármán, T. and Burgers, J.M., "General Aerodynamic Theory—Perfect Fluids," Vol. II of *Aerodynamic Theory,* edited by W.F. Durand, Dover Edition, New York, 1963.

AIAA 82-4218

Estimation of the Number of In-Flight Aircraft on Instrument Flight Rules

Norman Meyerhoff* and Jeffrey Garlitz†
U.S. Department of Transportation, Cambridge, Mass.

Introduction

MATHEMATICAL models to estimate the instantaneous aircount (IAC) of aircraft on instrument flight rules (IFR) over the United States have been developed. IAC is required to help plan for new or augmented air traffic control (ATC) computers which process information on these aircraft in real-time.

An economical method to estimate IAC is required because it is prohibitively costly to process radar target reports, which, prior to this research, had been the standard way to count aircraft.[1] IAC, which is defined to be the number of in-flight aircraft at any instant of time in any single day, are estimated by new models which convert (nonradar) aggregate data on landings and takeoffs to IAC.

The IAC of IFR aircraft are estimated for each air route traffic control center (ARTCC, or simply center), of which there are 20 covering the continental airspace. The IAC are also forecast,[2] although this Note will be limited to a summary of a pilot study to compare current IAC predictions with field data. IFR aircraft consist of scheduled aircraft (air carriers and air taxis) and unscheduled aircraft [general aviation (GA) aircraft].

Description of Models

The principal input to the scheduled model is the Official Airline Guide (OAG) tape, produced by the R.H. Donnelley Corporation. For each flight in the U.S., a great circle path is projected between the origin and destination to compute the location of an aircraft during specified intervals (in distance) of its flight. The aircount for a particular ARTCC and time of day is computed as follows. First, the scheduled departure and arrival times of each flight are examined to determine that the aircraft is in flight at the specified time of day (i.e., the time of day occurs between the departure and arrival times). Once it is established that the aircraft is in flight, the location of the flight at the particular time is computed, and if the aircraft's position (latitude, longitude) is determined to be over the relevant ARTCC, the aircount is incremented. Otherwise, the model examines the next flight from the OAG data using the same criteria. The model accesses a data base containing the boundaries of the ARTCCs, in the form of latitude and longitude, to determine which ARTCC the aircraft is passing over at a particular time of its flight.

There does not exist one easily accessible source of information for unscheduled aircraft operations. This would greatly complicate the problem were it not for the fact that the number of GA aircraft leaving an ARTCC is about equal to the number arriving, which means that only the number of IFR GA departures need be known to estimate the in-flight

Received Feb. 12, 1982. This paper is declared a work of the U.S. Government and therefore is in the public domain.

*Operations Research Analyst and Project Leader, Office of Air and Marine Systems, Operations Analysis Branch, U.S. Department of Transportation.

†Operations Research Analyst, Office of Air and Marine Systems, Operations Analysis Branch, U.S. Department of Transportation.

AUTHORS' NOTE: The views expressed in this Note are those of the authors but not necessarily those of the Department of Transportation or Federal Aviation Administration.